J Mol Model (2011) 17:2353–2366
DOI 10.1007/s00894-011-0986-7

ORIGINAL PAPER

Modeling of ligand binding to G protein coupled receptors: cannabinoid CB_1, CB_2 and adrenergic β_2AR

Dorota Latek · Michal Kolinski · Umesh Ghoshdastider · Aleksander Debinski · Rafal Bombolewski · Anita Plazinska · Krzysztof Jozwiak · Slawomir Filipek

Received: 20 October 2010 / Accepted: 24 January 2011 / Published online: 2 March 2011

Abstract Cannabinoid and adrenergic receptors belong to the class A (similar to rhodopsin) G protein coupled receptors. Docking of agonists and antagonists to CB_1 and CB_2 cannabinoid receptors revealed the importance of a centrally located rotamer toggle switch and its possible participation in the mechanism of agonist/antagonist recognition. The switch is composed of two residues, F3.36 and W6.48, located on opposite transmembrane helices TM3 and TM6 in the central part of the membranous domain of cannabinoid receptors. The CB_1 and CB_2 receptor models were constructed based on the adenosine A_{2A} receptor template. The two best scored conformations of each receptor were used for the docking procedure. In all poses (ligand-receptor conformations) characterized by the lowest ligand-receptor intermolecular energy and free energy of binding the ligand type matched the state of the rotamer toggle switch: antagonists maintained an *inactive* state of the switch, whereas agonists changed it. In case of agonists of β_2AR, the (*R,R*) and (*S,S*) stereoisomers of fenoterol, the molecular dynamics simulations provided evidence of different binding modes while preserving the same average position of ligands in the binding site. The (*S,S*) isomer was much more labile in the binding site and only one stable hydrogen bond was created. Such dynamical binding modes may also be valid for ligands of cannabinoid receptors because of the hydrophobic nature of their ligand-receptor interactions. However, only very long molecular dynamics simulations could verify the validity of such binding modes and how they affect the process of activation.

Keywords Cannabinoid receptors · Docking · Fenoterol · GPCRs · Molecular dynamics · Molecular switches

Electronic supplementary material The online version of this article (doi:10.1007/s00894-011-0986-7) contains supplementary material, which is available to authorized users.

D. Latek · U. Ghoshdastider · A. Debinski · S. Filipek (✉)
Faculty of Chemistry, University of Warsaw,
ul. Pasteura 1,
02-093 Warsaw, Poland
e-mail: sfilipek@chem.uw.edu.pl

M. Kolinski · A. Plazinska · K. Jozwiak
Department of Chemistry, Medical University of Lublin,
ul. Staszica 6,
20-081 Lublin, Poland

U. Ghoshdastider
Centre for Biomolecular Magnetic Resonance,
Institute for Biophysical Chemistry,
Goethe-University of Frankfurt/Main,
60438 Frankfurt/Main, Germany

R. Bombolewski
Faculty of Physics, University of Warsaw,
ul. Hoża 69,
00-681 Warsaw, Poland

D. Latek
International Institute of Molecular and Cell Biology,
ul. Ks. Trojdena 4,
02-109 Warsaw, Poland

Introduction

Recent crystal structures of class A (rhodopsin-like) G protein coupled receptors (GPCRs), namely β_1- and β_2-adrenergic receptors (β_1AR [1] and β_2AR [2–4]) and adenosine receptor (A_{2A}R [5]), showed nearly identical structures of transmembrane domains but also differences in the states of molecular switches as compared to rhodopsin [6] which was the first GPCR crystallized. Based on experimental data it was proposed that agonist binding and receptor activation occur through a series of conformational intermediates.

Transition between these intermediate states involves disruption, creation or reorganization of intramolecular interactions that stabilize the basal state of a receptor. These changes are elicited by the action of molecular switches (also called micro-switches). The major switches proposed so far for different GPCRs, reflecting shared activation mechanisms, include the "rotamer toggle switch" involving the CWxPx(F/H) sequence on TM6 [7], the switch based on the NPxxY $(x)_{(5,6)}$F sequence linking TM7 and H8 [8], and the "ionic lock" linking transmembrane helices TM3 and TM6 and employing the (E/D)RY motif on TM3. There are also switches not assigned to any particular sequence motifs like the "3-7 lock" involving the interaction between TM3 and TM7 and present only in selected receptor types: this switch involves Schiff base-counterion interaction in rhodopsin [9, 10] and it was proposed to operate in opioid receptors [11–13].

In the structure of rhodopsin which is completely inactive in the basal state, i.e., when retinal is in 11-*cis* conformation, all switches are assumed to be in their *off* positions. However, recent crystal structures of GPCRs, assumed to be in an *inactive* state because they were complexed with antagonists and inverse agonists, revealed that the states of switches were remarkably different from those of inactive rhodopsin: ionic lock was in an open state (broken connection between helices TM3 and TM6), and a connection between TM7 and H8 was broken because of a change of the rotamer of Y7.53 (part of NPxxY motif on TM7). On the other hand, the "rotamer toggle switch" involving W6.48 residue remained in its *off* state (identical as in inactive rhodopsin structure) in all receptor crystal structures even in the Meta-II rhodopsin structure assumed to be in *activated* form [14, 15]. Therefore, based on the existing crystal structures, different states of switches may not reflect the *on* and *off* positions but rather different states adopted during the activation process because these receptors may be partially activated in their basal state. In our earlier papers we investigated early activation steps occurring simultaneously to ligand binding in opioid receptors MOR (mu), DOR (delta) and KOR (kappa). The first switch that was broken by agonist binding was the "3-7 lock", a hydrogen bond D3.32-Y7.43 linking transmembrane helices TM3 and TM7. It was the first activation event observed. We also detected the action of a second switch: a rotamer toggle switch involving simultaneous change of side chain conformations of W6.48 and adjacent residues, therefore called the extended toggle switch. In the case of opioid receptors the other residue in this extended switch was H6.52. This residue also participated in the agonist-antagonist sensor as judged by the propensity for creating a hydrogen bond with Y3.33 for antagonists and H6.52 for agonists. All studied ligands, being analogs of morphine – with a common tyramine structural scaffold, created a salt bridge with D3.32 with their protonated nitrogen atom of the tyramine group. This sensor was studied by us for MOR [13] and later for DOR and KOR [12]. The proposed mechanism of its action was later confirmed via molecular dynamics simulations of a closely related agonist-antagonist pair of KOR ligands: 5'- and 6'-GNTI [11].

Ligands of opioid receptors are similar to ligands of β_1- and β_2-adrenergic receptors because they interact at the binding site of the receptor in a protonated form. This is not the case for ligands of cannabinoid receptors because of their hydrophobic properties. Following our earlier research on opioid receptors, where we proposed the location of an agonist-antagonist sensor, we investigated early activation steps in CB_1 and CB_2 receptors focusing on the centrally situated rotamer toggle switch involving residues W6.48 and F3.36 located on two different helices. Here we show our latest results on cannabinoid receptors CB_1 and CB_2 regarding the binding of ligands and possible activation steps simultaneous to ligand binding. Ligands of cannabinoid receptors are mostly hydrophobic as reflected by the presence of a large number of hydrophobic residues in the binding sites of their receptors. Therefore, the microswitches may be modified but they are still operational according to the structural mimicry rules. Identification of the agonist-antagonist sensor for ligands of cannabinoid receptors using simulation techniques is more difficult because their structures are usually highly flexible. Therefore, we decided to start with a simple docking method engaging flexible amino acid residues. This method was used to check the possibility whether the W6.48/F3.36 rotamer toggle switch may participate in the mechanism of agonist/antagonist sensor.

We also show our results regarding interactions between β_2-adrenergic receptor (β_2AR) model and two enantiomers of fenoterol, (*R*,*R*)-fenoterol and (*S*,*S*)-fenoterol, investigated by molecular dynamics (MD) simulations. Fenoterol is a selective β_2AR agonist and exists in four stereoisomers which significantly differ in β_2AR efficacies and selectivities. A racemic mixture of (*R*,*R*)- and (*S*,*S*)- isomers, *rac*-fenoterol, is used clinically for the treatment of asthma. Radioligand binding studies evidence that fenoterol stereochemistry greatly influences the binding affinity to β_2AR with the relative order: (*R*,*R*)>(*R*,*S*)>(*S*,*R*)>(*S*,*S*); a similar trend was found in functional assays [16]. Moreover, fenoterol stereochemistry also affects the mode of coupling of activated β_2AR to G proteins studied in experiments with pertussis toxin, a selective blocker of G_i mediated signaling. In these experiments the toxin had no effect on the activity of the (*R*,*R*)-fenoterol which indicates that this stereoisomer activates the receptor to associate exclusively with the G_s protein [17]. When other stereoisomers of fenoterol were tested in those experiments, the addition of pertussis toxin significantly reduced the functional effect implying that binding of non (*R*,*R*)- stereoisomers activates β_2AR to the form which interacts with both G_i and G_s protein [17].

Methods

Molecular models of human cannabinoid receptors CB_1 and CB_2 were prepared by a combined strategy joining Modeller [18], Rosetta-*ab-initio* [19] and Rosetta-loop-modeling [20]. In the first stage, we performed multiple alignments of sequences derived from cannabinoid receptors and available from the GPCR template structures: bovine rhodopsin, human β_2-adrenergic receptor, turkey β_1-adrenergic, human A_{2A} adenosine receptor (protein codes from Protein Data Bank: 1U19, 2RH1, 2VT4, 3EML, respectively). Multiple sequence alignments were prepared by two commonly used tools: MUSCLE [21, 22] and CLUSTALW (version 2.0) [23]. Both methods gave similar results. The highest pairwise sequence score according to CLUSTALW (based on normalized identity) was achieved for: CB_1-$A_{2A}R$ (24%), CB_2-β_1AR (22%) and also for CB_1-β_1AR and CB_2-$A_{2A}R$ (21%) pairs. Pairwise sequence score with rhodopsin was very low, 15% (CB_2) and 13% (CB_1), the same with β_2AR: 18% (CB_2) and 14% (CB_1). Consequently, we decided to choose structures of $A_{2A}R$ and β_1AR, both bound to antagonists in their crystal structures, as templates for homology modeling of CB_1 and CB_2. Alignment input for Modeller was prepared automatically by MUSCLE and adjusted manually in the Seaview editor [24] to preserve important functional motifs and disulfide bridges. Both CB_1 and CB_2 receptors have a single disulfide bridge located in the EC2 loop (both cysteins are within this loop: 257-264 in CB_1 and 174-179 in CB_2) [25] so the sequences of cannabinoid receptors were manually aligned with $A_{2A}R$ and β_1AR templates within the EC2 area to put cysteine residues in proximity. The final alignments for both templates are shown in Fig. S1 in supplementary material.

The transmembrane parts of the receptors were prepared by model-building routine in Modeller employing stereochemical parameters in CHARMM22 forcefield with subsequent MD-slow refinement of short loops. For the final assessment of the models we chose the discrete optimized protein energy (DOPE) option in Modeller, which is a pseudo-energy term based on a distance-dependent statistical potential [26]. The physics-based force fields are able to identify the correct models when starting structure is only very close to the native state (<0.15 nm). In the case presented in this paper, which is a hard homology modeling with the template-target sequence identity below 30%, the statistical potentials have the greatest ability to differentiate between models [18]. The mean DOPE score for 10 generated models was: -43281.0 (CB_1 based on A_{2A}), -42440.2 (CB_1 based on β_1AR), -38421.2 (CB_2 based on A_{2A}) and -37946.3 (CB_2 based on β_1AR). These scores reflect primarily the interactions within the bundle of transmembrane helices which are responsible for stabilization of the receptor. As the models based on $A_{2A}R$ were scored much better, we chose them for further docking studies. Subsequently, the Rosetta-loop-modeling protocol was used for remodeling the longest loop (IC3 – between helices TH5 and TM6): residues 300-335 in CB_1 and residues 217-234 in CB_2. Additionally, the N- and C-terminal parts of receptors, which are located outside the membrane, were modeled separately by the Rosetta-*ab-initio* protocol and joined with the rest of the protein by Modeller. The two final models of each receptor with the highest scores according to the DOPE measure were subjected to further analysis. We used these two conformations per each CB receptor to assess whether the choice of the model from the Modeller-generated ensemble influences the docking results to any extent.

To prove that the obtained models are stable and functional and can be used for ligand docking we analyzed the change of the cannabinoid receptors structure during short 1 ns molecular dynamic (MD) simulations in IMM1 [27] (a method in CHARMM program [28] with implicit membrane). However, because of a lack of explicit membrane (friction is diminished) the real length of this simulation was much longer. We conducted five simulations for CB_1 and six for CB_2 each time using different structures being the best scored receptor models based on the $A_{2A}R$ template from Modeller. The RMSD on C-alpha atoms was 0.27 nm for the transmembrane part of CB_1 and 0.18 nm for CB_2 on average. The representative plots of χ_1 angle for residues in the rotamer toggle switch (F3.36 and W6.48) are shown in Fig. S2 in supplementary material. The residues are stable although in some cases (Fig. S2b and d) the changes reflecting the spontaneous action of the switch were observed. This indicates that the models of CB_1 and CB_2 receptors we used were functional at least in the area of the binding site which is enough for ligand docking.

For the CB_1 and CB_2 receptor models, which were based on the $A_{2A}R$ template, we performed further studies, involving flexible docking of two antagonists (AM-630 and NESS-0327) and two agonists (anandamide (AEA) and (-)-Δ^9-THC) (Fig. 1). Input conformations of ligands were prepared using the LigPrep protocol from the Schrodinger Suite [29]. To sample different protonation states of ligands in physiological pH we used the Epik module [30]. From our set of ligands of CB_1 and CB_2 receptors, only AM630 was used in the protonated state (protonated nitrogen atom in morpholine ring) based on pK_a calculations (6.2±0.6). Since literature data [31] provide unequivocal evidence on this protonation, we decided to dock both forms of AM630. The obtained poses (positions and conformations of ligands in the receptor binding site) were similar, however, the protonated AM630 poses were characterized with higher energy values. Docking of all ligands were performed by

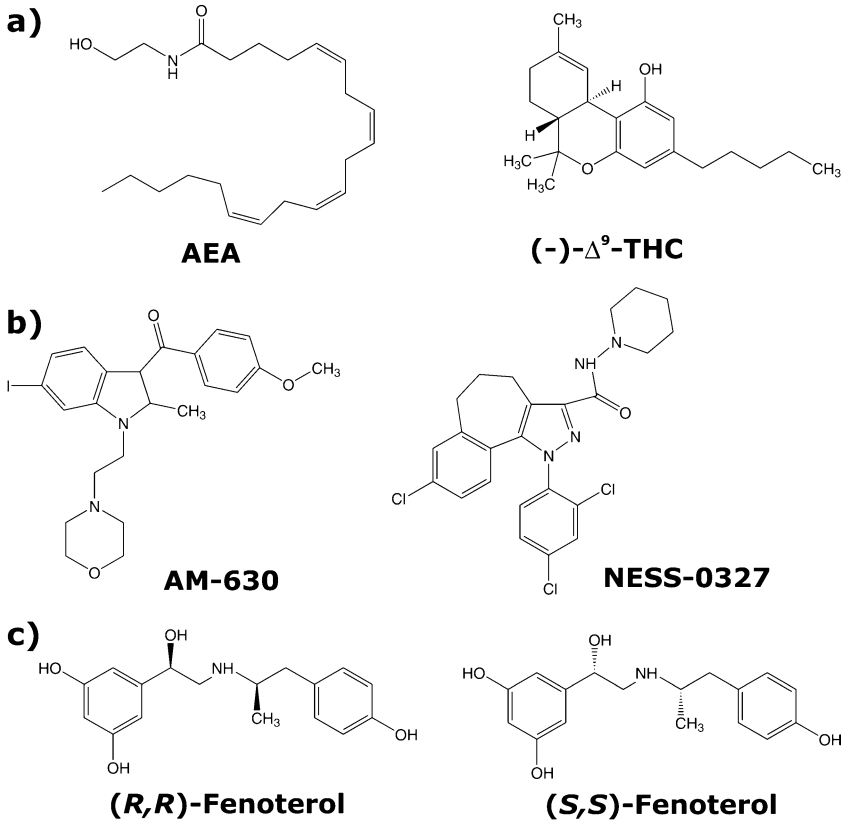

Fig. 1 Agonists (**a**) anandamide (AEA) and (-)-Δ^9-THC) (both unselective for CB_1 and CB_2), and antagonists (**b**) AM630 (CB_1 selective) and NESS-0327 (CB_2 selective) used in the study. (**c**) (*R,R*)- and (*S,S*)-fenoterol - agonists of β_2AR

Autodock 4.2 [32] using the genetic algorithm (GA) procedure. The following parameters for GA were used: 1.9 nm-large (50 grid points) search box, 150 individuals (poses - ligand/receptor conformations) in each population, 20 independent populations per each analyzed system (ligand-receptor complex), 2,500,000 energy evaluations per single evolution run, post-docking cluster analysis and other default settings. Some amino acids were set flexible during the docking. For this we chose amino acids with bulky residues close to the potential binding site (based on literature data): L3.29$^{(193)}$, V3.32$^{(196)}$, F3.36$^{(200)}$, F268 (EC2 loop), E5.37$^{(273)}$, F5.42$^{(278)}$, T5.47$^{(283)}$, W6.48$^{(356)}$, L6.51$^{(359)}$, L6.52$^{(360)}$, C7.42$^{(386)}$ for CB_1, and T3.33$^{(114)}$, F3.36$^{(117)}$, F183 (EC2 loop), D5.38$^{(189)}$, S5.42$^{(193)}$, I5.47$^{(198)}$, F5.51$^{(202)}$, W6.48$^{(258)}$, V6.51$^{(261)}$, L6.52$^{(262)}$, M6.55$^{(265)}$ for CB_2 receptor. Numbers of residues according to the Ballesteros-Weinstein numbering scheme [33] in which x.50 denotes the most conserved residue in each helix). To check the stability of ligand-receptor complexes we performed MD simulations of all complexes in explicit POPC membrane in YASARA program (YASARA Biosciences) using AMBER03 forcefield [34]. The periodic box contained about 120,000 atoms. The simulations were conducted in constant temperature 298 K (Berendsen thermostat) and a constant pressure 1 bar. The simulation time step was set 2 fs because of constraining of all bonds and the length of simulations was 5.5 ns. During the first 0.25 ns of simulation the complex was frozen to allow the membrane to relax and not disrupt the structure of the complex. The RMSD plots of all studied complexes of cannabinoid receptors are shown in Fig. S3 in supplementary material. Both the transmembrane part and the residues forming the binding site stabilized very quickly after the simulations started (about 0.5 ns) and were stable during the whole simulation.

Building of the complete structure of β_2AR was done on the basis of the crystal structure of human β_2AR-T4 lysozyme fusion protein with bound carazolol (PDB ID: 2RH1) [2]. Modeling of the N- and C-terminal domains of the receptor (residues 1-30 and 341-413) was conducted using a I-TASSER server [35]. The structure of the longest second intracellular loop of the receptor (residues 230-266) was predicted using the CABS program [36]. Single palmitoyl chain was added to C341 at the end of the cytoplasmic helix H8. Obtained β_2AR model was inserted into equilibrated palmitoyl-oleoyl-phosphatidylcholine (POPC) cell membrane model by means of the Inflategro procedure [37]. Model of β_2AR embedded in POPC lipid bilayer was then solvated with water molecules and ions were added. Energy minimization was conducted applying 2000 steps of the steepest descent algorithm followed by 2000 steps of the L-BFGS algorithm. Then, the molecular dynamic (MD) simulation lasting 40 ns was performed using the GROMACS (v. 3.3) program [38]. All calcu-

lations were conducted using modified GROMOS96 force field (ffG53a6 parameters set) [39] with additional parameters for POPC molecules [40]. SPC water model [41] was used and the PME procedure [42] was applied for treatment of the long-range electrostatic interactions. All bonds with hydrogen atoms were constrained by the LINCS algorithm [43]. MD was performed at the temperature of 310 K, pressure of 1 bar, and simulation time step was set at 1 fs.

To obtain the (*R,R*)- and (*S,S*)-fenoterol isomer structures and force field parameters for MD simulation the PRODRG server [44] was used. Geometry optimization of the two ligands in their protonated-nitrogen forms was completed using the Hartree–Fock procedure employing the 6–31G* basis set in Gaussian (v.03 rev. C.02, Gaussian Inc.). Partial charges for two molecules were obtained using the R.E.D. III procedure. In the first step, the molecular electrostatic potential (MEP) was calculated for the two fenoterol isomers. Then, the RESP method was used for fitting atom-centered charges according to the MEP of modeled ligands. The ligands were inserted in the middle of the binding site of the β_2AR model to preserve the interaction between D3.32 and the protonated amine nitrogen of ligands. To investigate differences in the binding of (*R,R*)- and (*S,S*)-fenoterol isomers similar starting structures of the two receptor-ligand complexes were generated during restrained MD simulation lasting 200 ps. Protein backbone atoms were constrained to their initial positions using the "freeze" option and weak harmonic distance restraints (the distance was 0.3 nm) were imposed on three receptor-ligand atom pairs (pair 1: C_γ atom of D3.32 residue and protonated nitrogen atom of ligand; pair 2: oxygen atom of hydroxyl group of S5.42 and oxygen atom of the first hydroxyl group of 1,3-benzenediol moiety; pair 3: oxygen atom of hydroxyl group of S5.46 and oxygen atom of second hydroxyl group of 1,3-benzenediol moiety). Finally, two step MD simulation of receptor-ligand complexes was preformed. During the first step, lasting 2 ns, weak harmonic position restraints were imposed only on the backbone atoms of transmembrane helices of the receptor and ligand-receptor distance restraints were released. In the second step the production run lasting 5 ns was conducted with no restraints. The two step MD simulation scheme described above was repeated 22 times, 11 times for receptor-(*S,S*)-fenoterol complex and also 11 times for receptor-(*R,R*)-fenoterol complex, applying random starting velocities for every atom. Simulation parameters were identical to those used for MD simulation of unliganded β_2AR model.

Results

To investigate the influence of ligand binding on amino acid residues at the binding site of CB_1 and CB_2 receptors to see a potential action of the rotamer toggle switch we used two conformations of cannabinoid receptors scored best by Modeller. These two conformations were similar to each other in the transmembrane domain but quite different in the extracellular loops area especially for the CB_2 receptor (Fig. 2). However, in all models, a phenylalanine residue located in EC2 is facing the core of the receptor forming a "hydrophobic cap" which makes the proposed models consistent with those proposed earlier [25]. Calculated root mean square distance (RMSD) between the two conformations of the CB1 and CB2 models was 0.258 nm and 0.265 nm, respectively (counting all heavy atoms in the receptor structure excluding N- and C-termini). Residues forming the rotamer toggle switch were located in the same positions whereas most of the other residues from the binding site adopted different conformations. For each pose of the ligand-receptor pair the free energy of binding and the ligand-receptor intermolecular energy were calculated. Intermolecular energy (E_{int}) is defined as the sum of four components: energies of van der Waals interactions, electrostatic interactions, hydrogen bonds and desolvation of the ligand. An error of E_{int} estimation is about 2.5 kcal mol^{-1}. ΔG is defined as the sum of E_{int} and the entropy term which is a change of entropy of a ligand and of a set of flexible amino acid side chains of a protein. The results obtained for two different conformations of each receptor are presented in Table 1. Usually ΔG and E_{int} had similar values with the exception of anandamide, which showed increased ΔG values owing to its flexibility. Nevertheless, the highly negative value of E_{int} in the case of AEA, as compared to other ligands, preserved a negative value of ΔG. Such exceptionally low value of intermolecular energy of anandamide inside the binding pocket of cannabinoid receptors is also associated with its flexibility resulting in the highest match with the amino acids from the binding site, especially hydrophobic ones. Regardless of the receptor conformation used, the poses with lowest E_{int} and ΔG were obtained for the ligands matching the rotamer switch state (involving residues W6.48 and F3.36): antagonists maintained the state of the rotamer toggle switch, whereas agonists changed it (values of E_{int} and ΔG in bold in Table 1). The poses were selected from two receptor conformations and two states of the switch as the ones with the lowest energy. The deviations from the pure *gauche+* and *trans* rotamers of W6.48 and F3.36 for χ_1 angle were high, usually about ±30º, and sometimes even higher, up to ±60º, which is half the way between pure *gauche+* and *trans* states.

For the best pose (characterized with the lowest energies E_{int} and ΔG) of the selective antagonist NESS-0327 in complex with CB_1 receptor (Fig. 3a) we observed the π-π aromatic interactions of the ligand with F268 residue. The piperidine ring of the ligand was located close to helices TM2 and TM7 while other rings in the area among helices

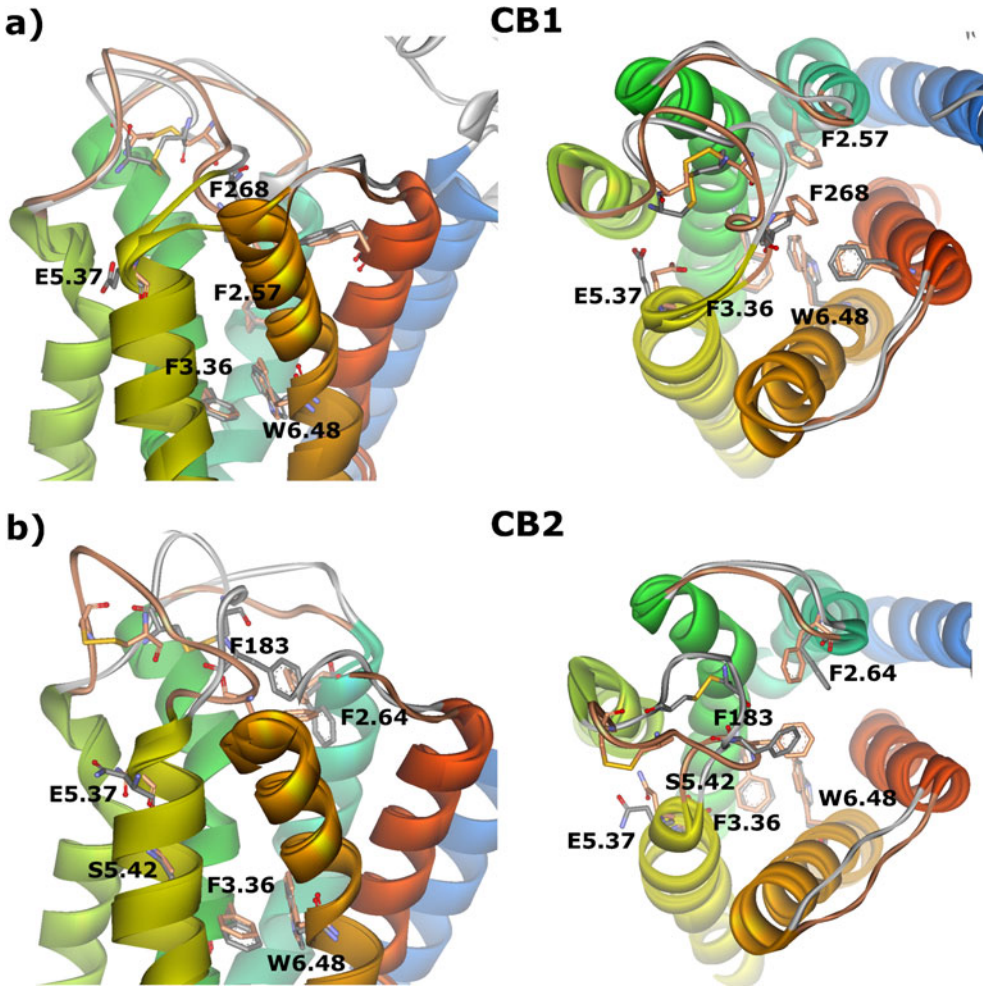

Fig. 2 Two views of the binding site, parallel to the membrane and from the extracellular side, of CB_1 (**a**) and CB_2 (**b**) receptors. The two best scored conformations for each receptor are superimposed. All presented models are based on the $A_{2A}R$ template. Residues forming the rotamer toggle switch and some characteristic residues of the binding site are shown

TMs:3-4-5-6. For the selective antagonist of CB_2, AM-630, we analyzed both the protonated and unprotonated form and got similar results of docking but slightly different energies of binding (Table 1). The protonated form tended to bind to conformation one of CB_2, while the unprotonated form to conformation two (although the energies for both conformations were very similar). Interestingly, the charged ligand was classified with higher energies than the ligand in unprotonated form for both receptor conformations. The ligand was bound to the receptor with the morpholine ring located close to the rotamer toggle switch area (Fig. 3b). The cation-π interaction was possible after a slight rotation of the phenyl ring (change of the χ_2 angle by 25º with no change of the χ_1 angle). An oxygen atom from the morpholine ring formed a hydrogen bond with S5.42$^{(193)}$, rather than S4.53$^{(161)}$ and S4.57$^{(165)}$ residues which are more distant to the ligand and covered partly by helix TM3. These serine residues in TM4 were important for binding of antagonist SR-144528 but not CP-55940 or WIN-55212-2 as pointed out by mutagenesis studies described in [45]. WIN-55212-2 contains a morpholine ring similarly to AM-630 and is also CB_2 selective. Interestingly, the serine residues, S4.53 and S4.57, are present only in CB_2 receptor so the other residue should be responsible for selectivity. According to mutagenesis studies done in Reggio group [46] such a residue is F5.46$^{(197)}$ and in fact in our model this residue is close to morpholine ring of AM-630. The anisole ring was located close to helices TM6 and TM7, while the iodobenzene ring close to helices TM3, TM4 and TM5. Among many analyzed poses of the antagonist AM-630 at the binding site of the CB_2 receptor one conformation appeared noteworthy due to a salt bridge formed by a protonated nitrogen atom of the morpholine ring of the ligand and the carboxylic group of E5.37 (not shown). Nevertheless, that pose was energetically less favorable (as scored by docking procedure). It means that appropriate hydrophobic interactions were a predominant feature of the best poses of this antagonist.

Binding of nonselective agonists (-)-Δ^9-THC and anandamide (AEA) changed the rotamers of the W6.48 and F3.36 residues in the rotamer toggle switch in both receptors (Fig. 4). In the CB_1 receptor an alkyl tail of AEA interacted with F268 (EC2 loop) through σ-π interactions. The polar part of AEA was located between

Table 1 The free energy of binding and intermolecular energy of the receptor-ligand complexes. The numbers in bold indicate the lowest energies for particular complexes and hence the most probable conformations of their structures

Complexes	Rotamer toggle switch state is matching the ligand type [a]				Opposite state of the switch to the ligand type			
	Conformation 1[b]		Conformation 2[c]		Conformation 1		Conformation 2	
	ΔG [d]	E_{int} [e]	ΔG	E_{int}	ΔG	E_{int}	ΔG	E_{int}
Antagonists								
NESS-0327 – CB_1	**-6.60**	**-7.50**	-3.93	-4.82	-2.16	-3.06	-4.28	-5.17
AM630(+) – CB_2	**-2.62**	**-4.41**	-1.91	-3.70	0.38	-1.41	3.73	1.94
AM630 – CB_2	-3.32	-5.11	**-3.37**	**-5.16**	-1.01	-2.80	-2.11	-3.90
Agonists								
AEA – CB_1	-0.01	-5.07	**-2.40**	**-7.47**	-0.34	-5.42	0.76	-4.32
THC – CB_1	-3.73	-5.23	**-4.54**	**-6.03**	-3.06	-4.55	-4.20	-5.69
AEA – CB_2	-3.90	-8.97	**-5.21**	**-10.28**	-1.71	-6.78	-3.33	-8.40
THC – CB_2	**-4.32**	**-5.81**	-3.82	-5.32	-1.70	-3.19	-2.27	-3.76

[a] Matching means *right-right* state of the switch for binding of antagonists and *left-left* state for binding of agonists (Fig. 6)

[b] The first of the two best receptor conformations generated by Modeller from the $A_{2A}R$ template

[c] The second of the two best receptor conformations generated by Modeller from the $A_{2A}R$ template

[d] Free energy of binding (calculated by Autodock) [kcal mol^{-1}]

[e] Intermolecular energy of the protein-ligand complex (calculated by Autodock) [kcal mol^{-1}] AM630(+) – protonated form of AM630

helices TMs:3-4-5, near the residues T3.33 and E5.37. The same location of the polar part of AEA was observed at the binding site of the CB_2 receptor, although the polar head of AEA was translated more toward TM4, possibly because TM4 in CB2 contains more polar residues (two serine residues S5.53 and S5.57 instead of alanine residues in CB_1). Additionally, a nitrogen atom in the polar head of AEA formed a hydrogen bond with S5.42. The alkyl tail of the ligand was elongated and its end was located in the hydrophobic pocket of CB_2 between TM2 and TM3 so it could interact with phenylalanine residues F2.61, F2.64, F3.25 and the hydrophobic part of K3.28 (charged part of

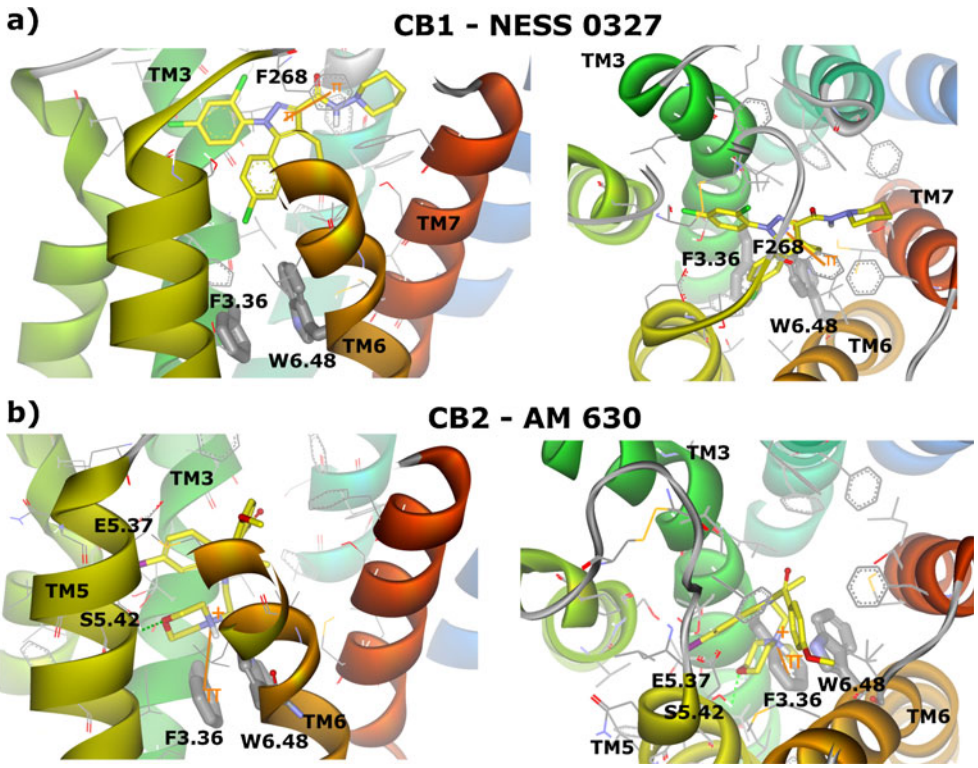

Fig. 3 Selective antagonists NESS-0327 and AM630 bound to CB_1 (**a**) and CB_2 (**b**) in complexes characterized by the lowest energies. Interactions involving π orbitals are shown as orange solid lines and hydrogen bonds as green dashed lines. Residues important for the binding of the ligand are shown

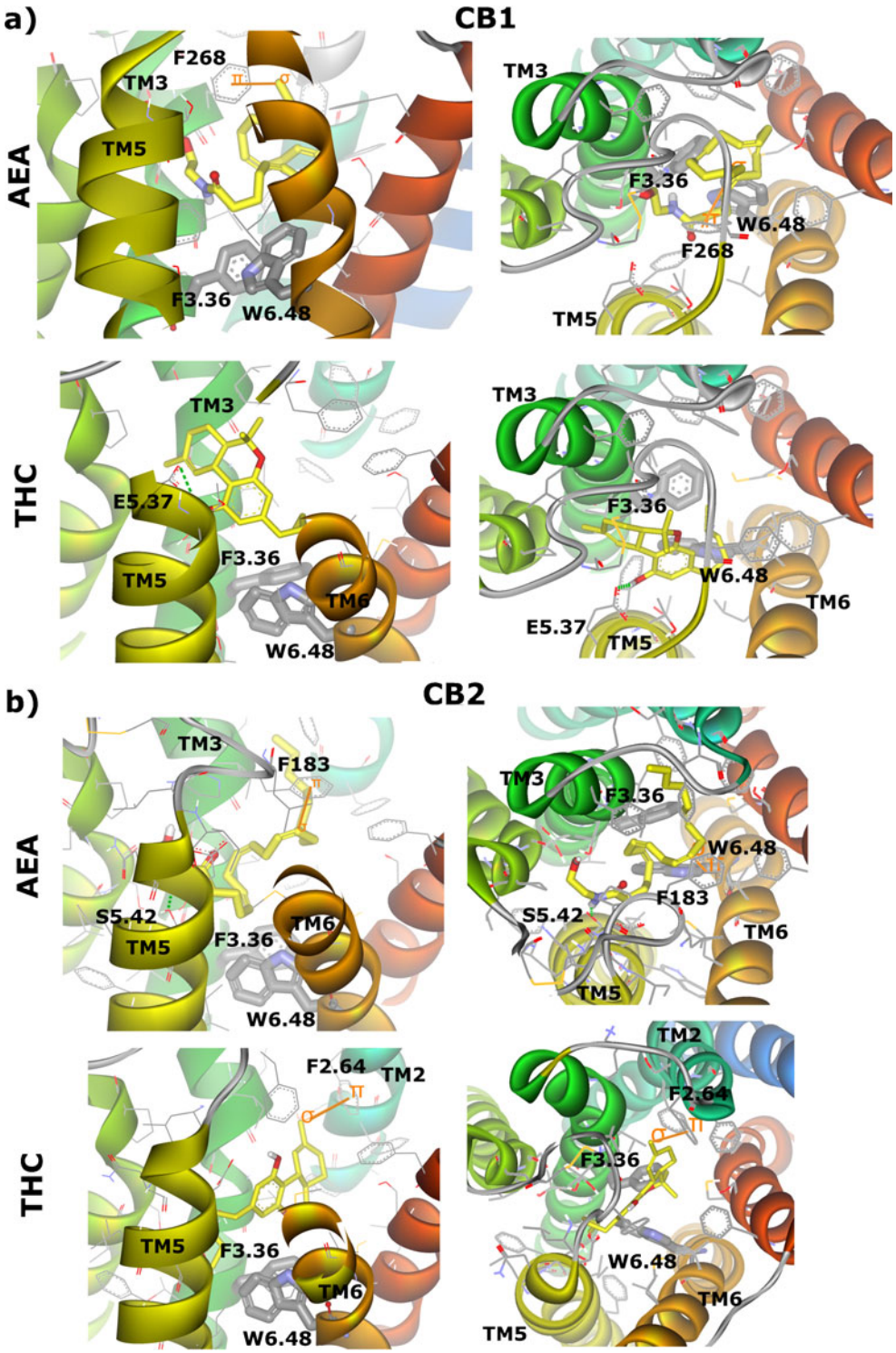

Fig. 4 Nonselective agonists (-)-Δ^9-THC and AEA bound to CB_1 (**a**) and CB_2 (**b**) in complexes characterized by the lowest energies. Interactions involving π orbitals are shown as orange solid lines and hydrogen bonds as green dashed lines. Residues important for the binding of the ligand are shown

this lysine residue projected outward of the receptor). The middle part of the tail of AEA interacted with F183 from the EC2 loop, similarly as in the AEA-CB_1 complex. Such interactions between phenylalanine in EC2 and CB_1 agonists was confirmed by mutagenesis in [25]. As regarding the other agonist, (-)-Δ^9-THC, its hydroxyl group formed a hydrogen bond with E5.37 in the THC-CB_1 complex, while its alkyl tail was located in the hydrophobic area between helices TMs:3-6-7 close to the rotamer toggle switch. In the THC-CB_2 complex the similar hydrogen bond was created between the hydroxyl group of a ligand and the carboxylic group of E5.37. The alkyl part of THC was located between helices TMs:3-5-6 of the receptor and also close to the switch, while the

opposite part of the ligand interacted with F2.64 (σ-π interactions).

For the analyzed β_2AR complexes with fenoterol the molecular dynamics simulations revealed different binding modes for the (*R,R*)- and (*S,S*)-fenoterol isomers. The starting positions of the two ligands were very similar. Two hydroxyl groups of ligand's 1,3-benzenediol moiety were located in the vicinity of the S5.42 and S5.46 residues of TM5, whereas ligand's protonated nitrogen atom was at a close distance to residues D3.32 of TM3 and N7.39 of TM7. During MD simulation of (*R,R*)-fenoterol the ligand's hydroxyl group located at the first stereogenic center formed hydrogen bonds with side chains of residues D3.32 and N7.39. The position of D3.32 side chain was also stabilized by interaction with Y7.43 residue in the TM7 helix. The hydrogen bond between the hydroxyl group of ligand's phenolic moiety and the D192 residue located in the EC2 loop was also well preserved during MD simulation. The two hydroxyl groups of ligand's 1,3-benzenediol moiety were oriented toward the S5.42 and S5.46 residues in TM5, but the distance was too large to form direct hydrogen bonds. In addition, the N6.55 residue, which is believed to play a crucial role in agonist binding and receptor activation [47], did not form any stable interaction with the ligand during MD simulation. In contrast to the (*R,R*) enantiomer, the (*S,S*)-fenoterol did not maintain a stable position at the receptor binding cavity. Only one well preserved contact was formed during each of the 11 MD simulations between the protonated nitrogen atom of (*S,S*)-fenoterol and the carboxyl group of the D3.32 residue. Interaction between the N7.39 residue and the ligand was temporarily established but frequently broken. The average distance between the hydroxyl group of the ligand phenolic moiety and the carboxyl group of D192 (EC2 loop) residue was too large (>0.45 nm) to establish a stable hydrogen bond. The movement of the ligand in the binding cavity allowed two hydroxyl groups of the 1,3-benzenediol moiety to move closer toward the S5.42 and S5.46 residues of TM5, but no stable connections were formed. Representative conformations of both the (*R,R*)- and (*S,S*)-fenoterol isomers were extracted from 22 MD simulations based on the lowest RMSD values when compared to the average position of the ligand observed during 5 ns MD trajectory. Superimposition of all extracted structures for each complex is shown in Fig. 5.

Discussion

Docking of agonists and antagonists to cannabinoid receptors revealed that the centrally located rotamer toggle switch can take part in agonist/antagonist differentiation and change its state simultaneously to ligand binding. The state of the switch was able to change even without a change of the backbone of the receptor, indicating its probable participation in early activation stages of the receptor. Following the structural mimicry principle in class A GPCRs one can identify this switch as a pair of residues W6.48/F3.36 in CB_1 and CB_2 cannabinoid receptors. These two residues located on two opposite helices, TM6 and TM3, are in contact with each other. Based on biochemical experiments McAllister et al. [48] highlighted the importance of this switch as a constraint for the CB_1-*inactive* state that may need to be broken during activation. Their modeling studies using inactive and fully activated CB_1 receptor models indicated that the W6.48/F3.36 contact can exist in the inactive state of CB_1 and be broken in the activated state via a chi1 (χ_1) rotamer switch: W6.48 (*gauche+*→*trans*) and F3.36(*trans*→*gauche+*). So it may represent a "toggle switch" for activation of CB_1. Our docking studies confirm their findings, however, because our modeling did not include movement of the backbone of helices one can regard this state as an early activation state of the receptor. In such a state there is still a partial interaction between residues W6.48 and F3.36 (Fig. 6) although they have adopted new positions enabling them to start rearrangement of adjacent residues through modification of the hydrogen bond network and to impose forces on adjacent helices for their subsequent displacement.

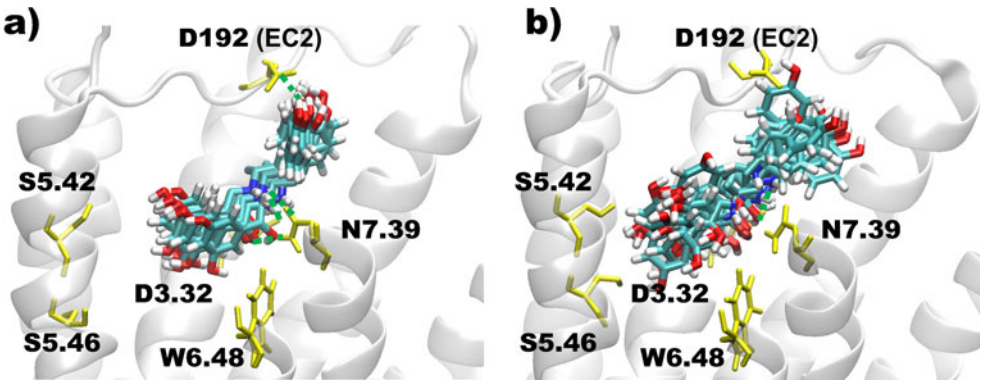

Fig. 5 Superimposition of representative ligand conformations extracted from 22 molecular dynamics simulations of the fenoterol-β_2AR complex; 11 conformations per each isomer of fenoterol: (*R,R*)-fenoterol (**a**), and (*S,S*)-fenoterol (**b**). Green dashed lines indicate hydrogen bonds

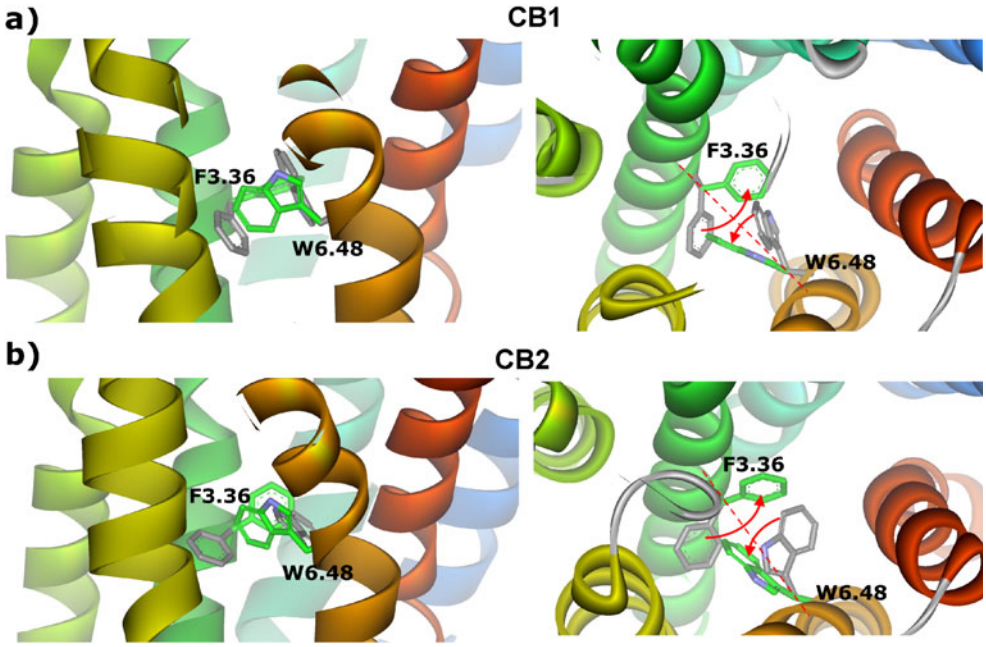

Fig. 6 The location of W6.48 and F3.36 residues (forming the rotamer toggle switch) in molecular models of CB_1 (**a**) and CB_2 (**b**) receptors viewed from the membrane (left panels) and from extracellular side (right panels). Residues in grey indicate so called *inactive* state (from complexes with antagonists), residues in green indicate *activated* state (from the complexes with agonists). Red arrows show the change in positions of W6.48 and F3.36 residues during the activation process. Based on location of these two residues with respect to the line connecting their C_β carbon atoms, viewed from extracellular side, one can identify the states of the switch as the *right-right* (*R-R*) state (both side chains in their right positions) or the *left-left* (*L-L*) state (both side chains in their left positions)

The presence of pure χ_1 *gauche+* and χ_1 *trans* rotamers of W6.48 and F3.36 was rare in the obtained poses especially for agonists of cannabinoid receptors: frequently the χ_1 angle deviated by about ±30º and sometimes (for the lowest energy pose of AEA-CB_1 complex) even by ±60º which is in between *gauche+* and *trans* states. This is possibly because of crowding in the binding site and the mismatch (which is a driving force for receptor activation) between the *inactive* structure of the receptor and docked agonists, as we analyzed the initial stages of activation by binding of all ligands to the receptor in the *inactive* state. Because of such discrepancies in the χ_1 angle of W6.48 and F3.36 residues, we decided to introduce another notation of the state of the switch indicating the mutual positions of the two residues in relation to each other. In this way the so called *inactive* state (present in the template and maintained by antagonists) is *right-right* (*R-R*), whereas the state preferred by agonists is *left-left* (*L-L*). The definition is based on the position taken by these two residues with regard to the line connecting their C_β carbon atoms viewed from the extracellular side (it is further explained and visualized in Fig. 6). The χ_2 angle of W6.48 and F3.36 residues was also able to change and helped to define the state of the switch: if a change of the χ_1 angle was not big enough to differentiate between *gauche+* and *trans* rotamers, then the location of the ring (via χ_2 angle - especially for W6.48) indicated the specific *R-R* or *L-L* state. Therefore, by incorporating the χ_1 and χ_2 angles, the proposed naming rule properly differentiated *inactive* and *activated* states of the rotamer toggle switch in the early stages of receptor activation. The conformations of the receptor for the best scored poses of the ligand-receptor complex were different but the switch was always in the *L-L* state for agonists while it was in the *R-R* state in the case of antagonists (the values in bold in Table 1). The poses with an opposite state of the switch (also obtained during docking procedure) were always classified with higher free energies and intermolecular energies. The docking procedure also provided *right-left* (*R-L*) and *left-right* (*L-R*) states of the switch among the docking results but all of them were of higher energy and are not shown.

The observations of the possible ligand poses in the cavity of cannabinoid receptors led us to the conclusion, that the van der Waals interactions are the most important for ligand binding while hydrogen bonds and even ionic interactions are less important. The highly scored poses (i.e., with the lowest energies) were often lacking strong hydrogen bonds (defined as donor-acceptor distance less than 0.25 nm), although some weak (donor-acceptor distance less than 0.45 nm [49]) could still be formed. The common interactions between the ligands and cannabinoid receptors involved π orbitals in phenyl rings, which are present in large quantities in the CB_1 and CB_2 receptors' binding sites, especially in the cavity between

helices TM2, TM7 and the EC2 loop (Figs. 3 and 4). For the most flexible ligand, AEA, about $5*10^6$ poses generated for each receptor conformation by the docking procedure ($2.5*10^5$ energy evaluations * 20 runs) was still too small a number to properly sample the conformational space of AEA even in the confined space of the receptor binding site. However, the fact that the *activated* state of the switch could be obtained for the lowest energy poses of this agonist indicates that such poses are not rare and may be dominant even for the *inactive* receptor structure that was used for docking.

In the computational studies Gonzalez et al. [50] preformed docking on a homology modeled CB_1 receptor. They docked WIN-55212-2 (agonist), SR-141716a (inverse agonist) and CP-55940 (non-classical agonist) ligands to CB_1 in a basal state and to the model of activated receptor obtained by translation and rotation of TM6. Docking results were similar to those obtained earlier by McAllister et al. [51] and confirmed preferential binding of ligands via two aromatic microdomains of CB_1 confined by helices TMs:3-5-6-7 and helices TMs:1-2-3-7. Docking revealed that all three ligands preferred the same binding site (TMs: 3-5-6-7), and only in the model of activated receptor (R*), one ligand, the non-classical agonist CP-55940, was docked to the second binding site. Another computational study on CB_1 and CB_2 receptors modeled on β_2AR and rhodopsin templates [52] revealed binding modes of the AMG3 ligand. Both templates proved to be useful and provided similar docking results. Aromatic residues were also an important part of the binding site. Shim et al. [53] conducted 105 ns molecular-dynamics simulations of empty CB_1 receptor embedded in POPC bilayer to obtain the structural and functional features of CB_1 over time. The helical bundle maintained a structure very similar to the x-ray structures of GPCRs. It was also revealed that the CB_1 receptor is stabilized by the formation of extensive, water-mediated hydrogen bond networks and aromatic stacking interactions within the helical core region. It is likely that these interactions, involving specific functional motifs, are the molecular constraints imposed on the inactive state of the CB_1 receptor. It was also suggested that disruption of these specific interactions is necessary to release the molecular constraints to achieve a conformational change of the receptor suitable for G-protein activation.

In the recent review of Shim [54] the initial stages of CB_1 receptor activation as well as the advantages of using of functional residues of CB_1 receptor for drug discovery are discussed based on accumulated biophysical and biochemical knowledge. The role of loops of CB_1 in ligand selection and binding was tested by Ahn et al. [25] based on alanine scanning mutagenesis of the EC2 loop. The aromatic residues F268 and F183 in CB_1 and CB_2 human cannabinoid receptors, respectively, are key residues in the C-X-X-X-Ar motif (where Ar is an aromatic residue) which is conserved in EC2 among GPCRs that bind biogenic amines and peptides. According to [25] the mutations of F268 in CB_1 displayed both impaired localization and ligand binding. Other amino acid substitutions at this position (F268N/Y/W) revealed that highly hydrophobic residues are required to accomplish both functions. Their findings are consistent with a dual role of EC2 loop in stabilizing receptor assembly and in ligand binding. The involvement of aromatic residue in the ligand binding of both CB_1 and CB_2 supports our docking results which are shown in Figs. 3 and 4.

Selectivity issues, i.e., how to develop compounds with high affinity for the CB_2 receptor and little affinity for the CB_1 receptor, are discussed in [55] for classical cannabinoids and cannabimimetic indoles. Interestingly, two opposite approaches, receptor mutations and molecular modeling, have been employed to obtain binding data. The selectivity of cannabinoid receptors was also investigated using molecular modeling and automated docking procedures [56]. Analysis of the interaction of WIN55212-2 with both receptors showed that CB_2/CB_1 selectivity is mainly determined by the interaction with the non-conserved residues S3.31 and F5.46 in CB_2 receptor. Importance of these residues was suggested by site-directed mutagenesis experiments.

Another type of selectivity involving coupling of β_2AR to G_s and G_i proteins was recently reported for fenoterol stereoisomers [17]. During MD simulations of β_2AR-fenoterol complexes we observed different binding modes for (*R,R*)- and (*S,S*)-fenoterol isomers which are in agreement with recent results from docking experiments [57]. (*R,R*)-fenoterol adopted a stable well preserved conformation inside the binding cavity and created a network of hydrogen bonds involving D3.32 and N7.39 residues. In contrast, the (*S,S*)-isomer showed much higher conformational flexibility. Interaction between ligand's protonated amine group and residue D3.32 was the only well preserved one during MD simulation. These findings can be important in explaining the differences between the β_2AR active states leading to G_s or G_s/ G_i selective coupling. W6.48 did not change its state during any of the 5 ns simulations possibly because of their short length. However, such length was enough to show critical differences in ligand binding modes of closely related compounds.

A number of conformational switches in β_2AR has been reported so far. The two best characterized are the R3.50-E6.30 ionic lock and W6.48 rotamer toggle switch. It was demonstrated that norepinephrine and dopamine break the ionic lock and engage the rotamer toggle switch whereas salbutamol, a noncatechol partial agonist, only breaks the ionic lock while the weak agonist catechol only engages the

rotamer toggle switch [58–62]. The activation mechanism is linked to the disruption of the network of interactions in the ionic lock. According to Romo et al. [62] the ionic lock can exist in three states: closed (or locked), semi-open with a bridging water molecule, and open. Recently Bokoch at al. [63] suggested that the extracellular domains of β_2AR also take part in the activation process. NMR spectroscopy and X-ray studies showed the functional role of the extracellular surface in ligand-specific conformational changes around the salt bridge linking D192 (EC2 loop) and K7.32 of β_2AR. This connection is formed in the unliganded β_2AR as well as in the complex with an inverse agonist – carazolol [1, 64] but certain agonists (including formoterol, a molecule structurally related to fenoterol) were reported to induce its breaking. Our results show that the (*R,R*)-fenoterol isomer forms well preserved interaction between the hydroxyl group of its phenolic moiety and the carboxyl group of the D192 (EC2 loop) residue during MD simulations in a similar manner as suggested by Bokoch et al. [63]. Such interaction has not been observed in simulations on the β_2AR - (*S,S*)-fenoterol complex.

The presence of the ionic lock switch is beyond question in nearly all GPCRs, however its impact on basal receptor activity is not obvious. Using D6.30N mutant of CB_1 and CB_2 receptors Nebane et al. [65] found that D6.30 is essential for full activation of both cannabinoid receptors. Both CB_1 and CB_2 D6.30N mutants demonstrated a level of constitutive activity not greater than that of their wild type counterparts, indicating that either D6.30 does not participate in a salt bridge with R3.50 (DRY motif), or the salt bridge is not critical for keeping cannabinoid receptors in the inactive conformation. The same conclusion was drawn from 2 μs simulations of empty β_2AR conducted to resolve the question of an open ionic lock in the crystal structure of this receptor with inverse agonist bound [66]. It turned out that the ionic lock in an empty receptor may or may not be open indicating two distinct *inactive* conformations of β_2AR in the basal state.

Conclusions

The flexible docking procedure for cannabinoid receptor CB_1 and CB_2 and molecular dynamics simulations for β_2-adrenergic receptor revealed significant differences in binding modes and provided additional insights into the activation processes of GPCRs. New structures of these receptors obtained as a result of progress in stabilization, overexpression and crystallization techniques will help explain to what extent the structural mimicry rule can be applied to GPCRs during activation processes. Longer molecular dynamics simulations, even reaching a millisecond timescale, will provide additional information about dynamics of the ligand-receptor complexes and possibly also about the course of the action of particular micro-switches. Taking into account the hypothesis of an ensemble of receptor conformations in the basal state one can also consider an ensemble of possible conformations of flexible ligands inside the binding site of the receptor. Such conformations, like that of anandamide in cannabinoid receptors and (*S,S*)-fenoterol in β_2AR, which lead to dynamical binding modes in the case of some ligand-receptor pairs, could also be investigated using simulations techniques.

Acknowledgments The work was supported by the Polish Ministry of Science and Higher Education (Grant no. N N301 2038 33) and by the Foundation for Polish Science (FOCUS and TEAM programmes). Publication supported by the European Union (Innovative Economy - European Regional Development Fund) grant no. POIG.02.03.00-00-003/09. We also acknowledge the computational grants no. G07-13 and G35-6 awarded by the Interdisciplinary Centre for Mathematical and Computational Modelling in Warsaw.

References

1. Warne T, Serrano-Vega MJ, Baker JG, Moukhametzianov R, Edwards PC, Henderson R, Leslie AGW, Tate CG, Schertler GFX (2008) Structure of a beta(1)-adrenergic G-protein-coupled receptor. Nature 454:486–491. doi:10.1038/nature07101
2. Cherezov V, Rosenbaum DM, Hanson MA, Rasmussen SGF, Thian FS, Kobilka TS, Choi HJ, Kuhn P, Weis WI, Kobilka BK, Stevens RC (2007) High-resolution crystal structure of an engineered human beta(2)-adrenergic G protein-coupled receptor. Science 318:1258–1265. doi:10.1126/science.1150577
3. Rosenbaum DM, Cherezov V, Hanson MA, Rasmussen SGF, Thian FS, Kobilka TS, Choi HJ, Yao XJ, Weis WI, Stevens RC, Kobilka BK (2007) GPCR engineering yields high-resolution structural insights into beta(2)-adrenergic receptor function. Science 318:1266–1273. doi:10.1126/science.1150609
4. Rasmussen SGF, Choi HJ, Rosenbaum DM, Kobilka TS, Thian FS, Edwards PC, Burghammer M, Ratnala VRP, Sanishvili R, Fischetti RF, Schertler GFX, Weis WI, Kobilka BK (2007) Crystal structure of the human beta(2) adrenergic G-protein- coupled receptor. Nature 450:383–387. doi:10.1038/nature06325
5. Jaakola VP, Griffith MT, Hanson MA, Cherezov V, Chien EYT, Lane JR, Ijzerman AP, Stevens RC (2008) The 2.6 angstrom crystal structure of a human A(2A) Adenosine receptor bound to an antagonist. Science 322:1211–1217. doi:10.1126/science.1164772
6. Palczewski K, Kumasaka T, Hori T, Behnke CA, Motoshima H, Fox BA, Le Trong I, Teller DC, Okada T, Stenkamp RE, Yamamoto M, Miyano M (2000) Crystal structure of rhodopsin: a G protein-coupled receptor. Science 289:739–745
7. Lei S, Liapakis G, Xu R, Guarnieri F, Ballesteros JA, Javitch JA (2002) beta(2) adrenergic receptor activation - modulation of the proline kink in transmembrane 6 by a rotamer toggle switch. J Biol Chem 277:40989–40996. doi:10.1074/jbc.M206801200
8. Fritze O, Filipek S, Kuksa V, Palczewski K, Hofmann KP, Ernst OP (2003) Role of the conserved NPxxY(x)(5, 6)F motif in the rhodopsin ground state and during activation. Proc Natl Acad Sci USA 100:2290–2295. doi:10.1073/pnas.0435715100
9. Porter JE, Hwa J, Perez DM (1996) Activation of the alpha(1b)-adrenergic receptor is initiated by disruption of an interhelical salt bridge constraint. J Biol Chem 271:28318–28323

10. Kim JM, Altenbach C, Kono M, Oprian DD, Hubbell WL, Khorana HG (2004) Structural origins of constitutive activation in rhodopsin: role of the K296/E113 salt bridge. Proc Natl Acad Sci USA 101:12508–12513. doi:10.1073/pnas.0404519101
11. Kolinski M, Filipek S (2010) Study of a structurally similar kappa opioid receptor agonist and antagonist pair by molecular dynamics simulations. J Mol Model 16:1567–1576. doi:10.1007/s00894-010-0678-8
12. Kolinski M, Filipek S (2009) Studies of the activation steps concurrent to ligand binding in DOR and KOR opioid receptors based on molecular dynamics simulations. TOSBJ 3:51–63. doi:10.2174/1874199100903010051
13. Kolinski M, Filipek S (2008) Molecular dynamics of mu opioid receptor complexes with agonists and antagonists. TOSBJ 2:8–20. doi:10.2174/1874199100802010008
14. Scheerer P, Park JH, Hildebrand PW, Kim YJ, Krauss N, Choe HW, Hofmann KP, Ernst OP (2008) Crystal structure of opsin in its G-protein-interacting conformation. Nature 455:497–502. doi:10.1038/nature07330
15. Park JH, Scheerer P, Hofmann KP, Choe HW, Ernst OP (2008) Crystal structure of the ligand-free G-protein-coupled receptor opsin. Nature 454:183–188. doi:10.1038/nature07063
16. Jozwiak K, Khalid C, Tanga MJ, Berzetei-Gurske I, Jimenez L, Kozocas JA, Woo A, Zhu W, Xiao RP, Abernethy DR, Wainer IW (2007) Comparative molecular field analysis of the binding of the stereoisomers of fenoterol and fenoterol derivatives to the beta2 adrenergic receptor. J Med Chem 50:2903–2915. doi:10.1021/jm070030d
17. Woo AY, Wang TB, Zeng X, Zhu W, Abernethy DR, Wainer IW, Xiao RP (2009) Stereochemistry of an agonist determines coupling preference of beta2-adrenoceptor to different G proteins in cardiomyocytes. Mol Pharmacol 75:158–165
18. Eswar N, Eramian D, Webb B, Shen MY, Sali A (2008) Protein structure modeling with MODELLER. Methods Mol Biol 426:145–159. doi:10.1007/978-1-60327-058-8_8
19. Rohl CA, Strauss CE, Misura KM, Baker D (2004) Protein structure prediction using Rosetta. Methods Enzymol 383:66–93. doi:10.1016/S0076-6879(04)83004-0
20. Mandell DJ, Coutsias EA, Kortemme T (2009) Sub-angstrom accuracy in protein loop reconstruction by robotics-inspired conformational sampling. Nat Methods 6:551–552. doi:10.1038/nmeth0809-551
21. Edgar RC (2004) MUSCLE: a multiple sequence alignment method with reduced time and space complexity. BMC Bioinform 5:1–19. doi:10.1186/1471-2105-5-113
22. Edgar RC (2004) MUSCLE: multiple sequence alignment with high accuracy and high throughput. Nucleic Acids Res 32:1792–1797. doi:10.1093/nar/gkh340
23. Larkin MA, Blackshields G, Brown NP, Chenna R, McGettigan PA, McWilliam H, Valentin F, Wallace IM, Wilm A, Lopez R, Thompson JD, Gibson TJ, Higgins DG (2007) Clustal W and clustal X version 2.0. Bioinformatics 23:2947–2948. doi:10.1093/bioinformatics/btm404
24. Gouy M, Guindon S, Gascuel O (2010) SeaView Version 4: a multiplatform graphical user interface for sequence alignment and phylogenetic tree building. Mol Biol Evol 27:221–224. doi:10.1093/molbev/msp259
25. Ahn KH, Bertalovitz AC, Mierke DF, Kendall DA (2009) Dual role of the second extracellular loop of the Cannabinoid receptor 1: ligand binding and receptor localization. Mol Pharmacol 76:833–842. doi:10.1124/mol.109.057356
26. Shen MY, Sali A (2006) Statistical potential for assessment and prediction of protein structures. Protein Sci 15:2507–2524. doi:10.1110/ps.062416606
27. Lazaridis T (2003) Effective energy function for proteins in lipid membranes. Proteins 52:176–192
28. Brooks BR, Brooks CL, Mackerell AD, Nilsson L, Petrella RJ, Roux B, Won Y, Archontis G, Bartels C, Boresch S, Caflisch A, Caves L, Cui Q, Dinner AR, Feig M, Fischer S, Gao J, Hodoscek M, Im W, Kuczera K, Lazaridis T, Ma J, Ovchinnikov V, Paci E, Pastor RW, Post CB, Pu JZ, Schaefer M, Tidor B, Venable RM, Woodcock HL, Wu X, Yang W, York DM, Karplus M (2009) CHARMM: the biomolecular simulation program. J Comput Chem 30:1545–1614
29. LigPrep, version 2.4: Schrödinger, LLC, New York; (2010)
30. Epik, version 2.1: Schrödinger, LLC, New York; (2010)
31. Reggio PH (2003) Pharmacophores for ligand recognition and activation/inactivation of the cannabinoid receptors. Curr Pharm Des 9:1607–1633
32. Morris GM, Huey R, Lindstrom W, Sanner MF, Belew RK, Goodsell DS, Olson AJ (2009) AutoDock4 and AutoDockTools4: automated docking with selective receptor flexibility. J Comput Chem 30:2785–2791. doi:10.1002/jcc.21256
33. Ballesteros JA, Weinstein H (1995) Integrated methods for the construction of three-dimensional models and computational probing of structure-function relations in G protein-coupled receptors. Methods Neurosci 25:366–428
34. Duan Y, Wu C, Chowdhury S, Lee MC, Xiong G, Zhang W, Yang R, Cieplak P, Luo R, Lee T, Caldwell J, Wang J, Kollman P (2003) A point-charge force field for molecular mechanics simulations of proteins based on condensed-phase quantum mechanical calculations. J Comput Chem 24:1999–2012. doi:10.1002/jcc.10349
35. Roy A, Kucukural A, Zhang Y (2010) I-TASSER: a unified platform for automated protein structure and function prediction. Nat Protoc 5:725–738. doi:10.1038/nprot.2010.5
36. Kolinski A (2004) Protein modeling and structure prediction with a reduced representation. Acta Biochim Pol 51:349–371
37. Kandt C, Ash WL, Tieleman DP (2007) Setting up and running molecular dynamics simulations of membrane proteins. Methods 41:475–488. doi:10.1016/j.ymeth.2006.08.006
38. Van der Spoel D, Lindahl E, Hess B, Groenhof G, Mark AE, Berendsen HJC (2005) GROMACS: fast, flexible, and free. J Comput Chem 26:1701–1718. doi:10.1002/jcc.20291
39. Oostenbrink C, Villa A, Mark AE, van Gunsteren WF (2004) A biomolecular force field based on the free enthalpy of hydration and solvation: the GROMOS force-field parameter sets 53A5 and 53A6. J Comput Chem 25:1656–1676. doi:10.1002/jcc.20090
40. Kukol A (2009) Lipid models for united-atom molecular dynamics simulations of proteins. J Chem Theory Comput 5:615–626. doi:10.1021/ct8003468
41. van der Spoel D, van Maaren PJ, Berendsen HJC (1998) A systematic study of water models for molecular simulation: derivation of water models optimized for use with a reaction field. J Chem Phys 108:10220–10230. doi:10.1063/1.476482
42. Darden T, York D, Pedersen L (1993) Particle mesh Ewald: an N·log(N) method for Ewald sums in large systems. J Chem Phys 98:10089–10092. doi:10.1063/1.464397
43. Hess B, Bekker H, Berendsen HJC, Fraaije J (1997) LINCS: a linear constraint solver for molecular simulations. J Comput Chem 18:1463–1472
44. Schuttelkopf AW, van Aalten DM (2004) PRODRG: a tool for high-throughput crystallography of protein-ligand complexes. Acta Crystallogr D Biol Crystallogr 60:1355–1363. doi:10.1107/S0907444904011679
45. Gouldson P, Calandra B, Legoux P, Kerneis A, Rinaldi-Carmona M, Barth F, Le Fur G, Ferrara P, Shire D (2000) Mutational analysis and molecular modelling of the antagonist SR 144528 binding site on the human cannabinoid CB(2) receptor. Eur J Pharmacol 401:17–25. doi:10.1016/S0014-2999(00)00439-8
46. Song ZH, Slowey CA, Hurst DP, Reggio PH (1999) The difference between the CB(1) and CB(2) cannabinoid receptors

at position 5.46 is crucial for the selectivity of WIN55212-2 for CB(2). Mol Pharmacol 56:834–840
47. Wieland K, Zuurmond HM, Krasel C, Ijzerman AP, Lohse MJ (1996) Involvement of Asn-293 in stereospecific agonist recognition and in activation of the beta(2)-adrenergic receptor. Proc Natl Acad Sci USA 93:9276–9281
48. McAllister SD, Hurst DP, Barnett-Norris J, Lynch D, Reggio PH, Abood ME (2004) Structural mimicry in class A G protein-coupled receptor rotamer toggle switches - the importance of the F3.36(201)/W6.48(357) interaction in cannabinoid CB1 receptor activation. J Biol Chem 279:48024–48037. doi:10.1074/jbc.M406648200
49. Jeffrey GA (1997) An introduction to Hydrogen bonding. Oxford University Press, Oxford
50. Gonzalez A, Duran LS, Araya-Secchi R, Garate JA, Pessoa-Mahana CD, Lagos CF, Perez-Acle T (2008) Computational modeling study of functional microdomains in cannabinoid receptor type 1. Bioorg Med Chem 16:4378–4389. doi:10.1016/j.bmc.2008.02.070
51. McAllister SD, Rizvi G, Anavi-Goffer S, Hurst DP, Barnett-Norris J, Lynch DL, Reggio PH, Abood ME (2003) An aromatic microdomain at the cannabinoid CB1 receptor constitutes an agonist/inverse agonist binding region. J Med Chem 46:5139–5152. doi:10.1021/jm0302647
52. Durdagi S, Papadopoulos MG, Zoumpoulakis PG, Koukoulitsa C, Mavromoustakos T (2010) A computational study on cannabinoid receptors and potent bioactive cannabinoid ligands: homology modeling, docking, de novo drug design and molecular dynamics analysis. Mol Divers 14:257–276. doi:10.1007/s11030-009-9166-4
53. Shim JY (2009) Transmembrane helical domain of the Cannabinoid CB1 receptor. Biophys J 96:3251–3262. doi:10.1016/j.bpj.2008.12.3934
54. Shim JY (2010) Understanding functional residues of the Cannabinoid CB1 receptor for drug discovery. Curr Top Med Chem 10:779–798
55. Poso A, Huffman JW (2008) Targeting the cannabinoid CB2 receptor: modelling and structural determinants of CB2 selective ligands. Br J Pharmacol 153:335–346. doi:10.1038/sj.bjp.0707567
56. Tuccinardi T, Ferrarini PL, Manera C, Ortore G, Saccomanni G, Martinelli A (2006) Cannabinoid CB2/CB1 selectivity. Receptor modeling and automated docking analysis. J Med Chem 49:984–994. doi:10.1021/jm050875u
57. Seifert R, Dove S (2009) Functional selectivity of GPCR ligand stereoisomers: new pharmacological opportunities. Mol Pharmacol 75:13–18. doi:10.1124/mol.108.052944
58. Yao XJ, Parnot C, Deupi X, Ratnala VRP, Swaminath G, Farrens D, Kobilka B (2006) Coupling ligand structure to specific conformational switches in the beta(2)-adrenoceptor. Nat Chem Biol 2:417–422. doi:10.1038/nchembio801
59. Ghanouni P, Gryczynski Z, Steenhuis JJ, Lee TW, Farrens DL, Lakowicz JR, Kobilka BK (2001) Functionally different agonists induce distinct conformations in the G protein coupling domain of the beta 2 adrenergic receptor. J Biol Chem 276:24433–24436. doi:10.1074/jbc.C100162200
60. Swaminath G, Xiang Y, Lee TW, Steenhuis J, Parnot C, Kobilka BK (2004) Sequential binding of agonists to the beta2 adrenoceptor. Kinetic evidence for intermediate conformational states. J Biol Chem 279:686–691. doi:10.1074/jbc.M310888200
61. Swaminath G, Deupi X, Lee TW, Zhu W, Thian FS, Kobilka TS, Kobilka B (2005) Probing the beta2 adrenoceptor binding site with catechol reveals differences in binding and activation by agonists and partial agonists. J Biol Chem 280:22165–22171. doi:10.1074/jbc.M502352200
62. Romo TD, Grossfield A, Pitman MC (2010) Concerted interconversion between ionic lock substates of the beta(2) adrenergic receptor revealed by microsecond timescale molecular dynamics. Biophys J 98:76–84. doi:10.1016/j.bpj.2009.09.046
63. Bokoch MP, Zou Y, Rasmussen SG, Liu CW, Nygaard R, Rosenbaum DM, Fung JJ, Choi HJ, Thian FS, Kobilka TS, Puglisi JD, Weis WI, Pardo L, Prosser RS, Mueller L, Kobilka BK (2010) Ligand-specific regulation of the extracellular surface of a G-protein-coupled receptor. Nature 463:108–112. doi:10.1038/nature08650
64. Hanson MA, Cherezov V, Griffith MT, Roth CB, Jaakola VP, Chien EYT, Velasquez J, Kuhn P, Stevens RC (2008) A specific cholesterol binding site is established by the 2.8 angstrom structure of the human beta(2)-adrenergic receptor. Structure 16:897–905
65. Nebane NM, Kellie B, Song ZH (2006) The effects of charge-neutralizing mutation D6.30N on the functions of CB1 and CB2 cannabinoid receptors. FEBS Lett 580:5392–5398. doi:10.1016/j.febslet.2006.09.001
66. Dror RO, Arlow DH, Borhani DW, Jensen MO, Piana S, Shaw DE (2009) Identification of two distinct inactive conformations of the beta(2)-adrenergic receptor reconciles structural and biochemical observations. Proc Natl Acad Sci USA 106:4689–4694. doi:10.1073/pnas.0811065106